IEEE Access
Multidisciplinary | Rapid Review | Open Access Journal

SPECIAL SECTION ON UNCERTAINTY QUANTIFICATION IN ROBOTIC APPLICATIONS

Received August 27, 2019, accepted October 25, 2019, date of publication November 15, 2019, date of current version December 4, 2019.

Digital Object Identifier 10.1109/ACCESS.2019.2953471

Robotic Arthroscopy: The Uncertainty in Internal Knee Joint Measurement

MARIO STRYDOM[1,2], ROSS CRAWFORD[1,2,3,4], JONATHAN ROBERTS[1,2,3], (Senior Member, IEEE), AND ANJALI JAIPRAKASH[1,2,3]

[1]Science and Engineering Faculty, Queensland University of Technology, Brisbane, QLD 4000, Australia
[2]Medical and Healthcare Robotics, Australian Centre for Robotic Vision, Brisbane, QLD 4000, Australia
[3]Institute of Health and Biomedical Innovation, Queensland University of Technology, Brisbane, QLD 4000, Australia
[4]The Prince Charles Hospital, Brisbane, QLD 4032, Australia

Corresponding author: Mario Strydom (mario.strydom@hdr.qut.edu.au)

This work was supported in part by the Advanced Queensland Scheme, in part by the Queensland University of Technology Research Training Program, and in part by the Cadaveric experiment through the Australian National Health and Medical Research Council (NHMRC) Committee EC00171 under Grant 1400000856.

ABSTRACT We report a study that developed algorithms to measure the dimension and uncertainty range of free space inside the knee joint for the purpose of minimally invasive surgery. During knee arthroscopy, the patient's leg position is continuously adjusted to create the space for surgical instruments inside the joint. Surgeons 'feel' the force they apply to the leg and estimate the joint space from a 2D video. In many cases, they overestimate the instrument gap, resulting in damaging to the knee joint by pushing instruments through a gap that is too small. We used cadaveric experiments to inform the noise induced by the sensors and image processing steps, to derive an error point-cloud in a simulated environment. From the point-cloud, we calculate the instrument gap range inside the knee joint. For a selected surgical instrument gap size, the measurement algorithm is accurate to less than a millimetre. However, measurement errors introduce an uncertainty of 14%. The performance of our algorithms demonstrates the use of a single-lens arthroscope to measure the instrument gap to provide feedback to a surgeon or enable control of a robotic leg manipulator.

INDEX TERMS Computer vision, joint motion stereo, image segmentation, optical tracking, error analysis, measurement uncertainty.

I. INTRODUCTION

Knee arthroscopy is a minimally invasive surgery (MIS) and is normally performed through two portals, as shown in Figure 1 [1]. Damage and recovery time for patients is significantly reduced when compared to open surgical techniques [2]. It is one of the most routinely performed minimally invasive orthopaedic procedures for diagnosing and repairing knee joint disorders [3].

Arthroscopes currently used by surgeons during arthroscopic surgery provide live video imagery of the internal knee geometry of the patient. The surgeon changes the leg angle and position to expose different parts of the inner knee to the arthroscopic camera [3]. Part of the internal structure of the knee is the ''instrument gap'', as seen in Figure 1a. It is a dynamic opening inside the knee that is adjusted through manipulation of the patient's leg (Figure 1b) until surgical tools can be guided through it [4]. The main objective of this study is to use in vivo experimental results and realistic simulation parameters to measure the instrument gap and develop algorithms that analyse the uncertainty of the measurement, by accounting for image and translational measurement errors. For control of leg motion, this uncertainty range needs to be sufficiently large for the arthroscope to pass through, and small enough not to reach the anatomical limits of the patient's joint [5] and cause unintentional damage when adjusting the leg.

The associate editor coordinating the review of this manuscript and approving it for publication was Zhonglai Wang.

A. PROBLEM DESCRIPTION

While knee arthroscopy is a common procedure, it requires a skilled and experienced surgeon to repair the damage to the knee joint ([6]). The procedure is challenging, and research shows that a safer environment can be created by providing feedback to the surgeon when moving the patient's leg [7]. Today there is no algorithm to measure the knee joint reliably,

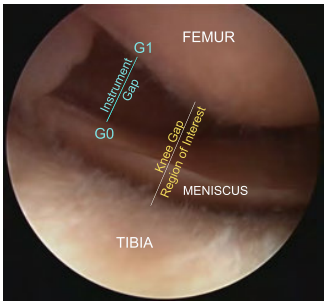

(a) Knee joint view during an arthroscopy. The Knee gap includes all the internal knee joint structures, while the instrument gap is the space surgical instruments can pass through.

(b) Surgeon manipulating the leg and steering the surgical instruments using the 2D arthroscope image on screen as guide.

FIGURE 1. **Knee minimal invasive surgery.**

and stereo systems used in other MIS surgeries are not suited for knee arthroscopy due to the small size of the arthroscope with only a single lens and the harsh environment inside the knee joint.

Although a few technologies such as deep learning can measure distance inside the body, it is necessary to consider the precision required and thus, the practical use of technology during an arthroscopic procedure. A surgeon or robot's (Operator) capability to manoeuvre the surgical instrument or 4mm arthroscopy through an instrument gap of zero to fifteen millimetres varies and affects the measurement technology and error tolerance range for safe navigation. For surgeons, factors such as experience, age and fatigue limit their ability to manoeuvre instruments through a gap seen on a 2D image. For robots, the manufacturing quality of links, gearboxes and controls determine how accurate they can steer an end effector such as an arthroscope.

For each surgical situation, the accuracy of the gap measurement needs to be of similar order as the operator capability range. Four million knee arthroscopies are performed annually and demand the increase in safety for patients and surgeons. This study addresses the significant challenge of measuring the instrument gap with a high level of precision for feedback to a robotic system or a surgeon.

B. ASSUMPTIONS

For this research, it is assumed that:

1) The standard arthroscope is used to capture images as it is used in over four million surgeries annually.
2) The joint is static between frames, which is typical as a surgeon normally pause between leg movements to determine if the gap is adequate.
3) The instrument gap can be reliably segmented from one image frame to another as shown by Strydom *et al.* [4].
4) To measure the instrument gap, a requirement is to accurately track the anatomical points of interest inside the knee joint that forms the instrument gap, which is beyond the scope of this study. Marmol *et al.* evaluated options for tracking feature inside the knee joint [8].

C. RELATED WORK

The visual feedback from the arthroscope is crucial for surgeons to observe internal body structures and navigate the instruments to the area under surgery [9]. Indeed, there is a burgeoning interest in visually guided robots to observe, understand and use video information in a medical environment. Computer Vision can be used to extract information from a variety of applications effectively. In the case of knee arthroscopy, vision-based algorithms are well placed to detect inner knee parameters and use this data to provide greater insight for surgeons.

Stereo vision [10] is today a common technique used to determine depth or distance measurements in medical applications, such as that used in the Stryker Mako system [11], [12]. Röhl *et al.* demonstrates how stereo endoscopes can aid the surgeon by providing real-time depth information to millimetre accuracy and detailed 3D reconstructions of the organs ([13]. Field *et al.* [14] used established algorithms to demonstrate how stereoscopes can restore the depth perception lost during MIS. Even though stereo hardware is available for specific MIS applications, only single-lens cameras (motion) is currently available for arthroscopy. Surgeons are relatively good at estimating depth from a two-dimensional image. However, it is a significant challenge to use a standard motion arthroscope camera [15] to measure the instrument gap.

Ye *et al.* [16] proposed depth estimation using stereo image pairs in a deep learning framework. For real-time measurement Visentini-Scarzanella *et al.* [17] used endoscopic imaging and CT imaging in a patient-specific deep learning network for bronchoscopy. Using a monocular bronchoscope, the system achieved an average accuracy of 1.5mm in an artificial silicone bronchial phantom. However, the study doesn't provide the variation or the impact of errors during a procedure on the measurement range. The knee is a further vastly more complex environment, and current results from deep learning show it is not a viable or practical technology to accurately (sub-millimetre) measure the dynamic and small space inside the knee joint.

Structure from motion (SfM) recovers camera motion and the 3D information using images captured over time for both stereo or monocular cameras as detailed by Chwa *et al.* [18] and Scaramuzza *et al.* [19]. SfM is typically slow; however, for this research, we only need to measure the instrument gap. Mazzon shows that estimation of a point using a single camera is higher than 96.4% in the x, y and z directions [20]. Yang *et al.* [21] developed an approach to estimate egomotion and vehicle distance using a monocular camera. Using motion stereo, we can calculate a range using two motion images from the arthroscope, where the egomotion is known between frames. By externally using optical tracking on the arthroscope, the motion of the internal lens position or arthroscope tip position can be calculated to a sub-millimetre precision [22]. Maletsky *et al.* shows the accuracy of motion (translation and rotation) to be smaller than 0.1 (mm or deg) for a 4m volume size [23]. Saxena *et al.* [24] used motion

cues and stereo information to increase the accuracy of range estimation, which can be a benefit in measuring the knee joint. Scaramuzza *et al.* [19] shows that for a single camera (as with the arthroscope), to know the absolute scale of a scene it is necessary to know the baseline of the camera motion or the size of at least one part of the scene. For this study, we use optical tracking on the arthroscope to get the absolute scale of the arthroscope translation.

While extensive research has been performed to determine the range to an object, well-defined error analysis for it is not comprehensive. Error analysis that has been researched in motion stereo include [25], [26]:

- Linear triangulation methods,
- The Midpoint method (the most common method) of estimating the actual distance from the two camera viewpoint rays
- Polynomial methods designed to find an optimal global solution in the presence of a noise model

The above methods are all approximations of the errors inside the error volume generated by the measurement discrepancies, such as with the Midpoint method, which was found not to be a good result [27]. However, we need greater insight into the errors introduced due to sensor measurements – specifically, the unique combination of errors in measuring the instrument gap during an arthroscopy.

In the case of MIS, it is essential to understand the error range in the uncertainty measurement of the knee joint to ensure the safety of the patient. This study presents a novel approach, where a point cloud is calculated from measurement errors to determine the measurement uncertainty of the instrument gap. The errors that are introduced include image segmentation and the translation and rotation of the arthroscope. Translation of the arthroscope is only a few millimetres inside the knee joint and with a frame-rate of 60 fps, allows a high number of frames to be translated for each one millimetre of movement. Fang *et al.* shows for motion vehicle systems that the distance (in meters) from 1 to 250 frames reduce from 0.6m to 0.1m [21] and that the forward velocity converges in less than 50 frames. However, current literature doesn't link translation of a motion camera to the changes of the measurement uncertainty, which forms part of this study.

D. CONTRIBUTIONS

Our novel approach uses a standard arthroscope and develops algorithms to make motion stereo a viable option to measure the knee joint. The contributions of this study are:

1) A computer vision algorithm to measure the instrument gap using motion stereo with optical tracking on the arthroscope.
2) The measurement errors for knee arthroscopy as measured from three cadaver arthroscopy experiments.
3) An algorithm and realistic simulations to calculate the error point-cloud and uncertainty in the instrument gap measurement.
4) An algorithm for the arthroscope translation distance to achieve a specific instrument gap.

From the literature and comparing measuring and 3D reconstruction technologies such as deep learning and structure from motion with motion stereo, it is clear that for arthroscopy, motion stereo is the best option to measure the knee joint cavity. To the best of our knowledge, this is the first study to measure the inside of the knee joint, identify arthroscopy measurement errors, calculate the uncertainty of the instrument gap opening. It allows feedback to a robotic leg manipulator, surgical robots or to a surgeon to have a better outcome for patients.

II. METHOD

The uncertainty in measuring the front, medial instrument gap will be analysed, and motion stereo used to calculate the instrument gap size. With this measurement, an error exists, and thus, specific errors for the knee joint during an arthroscopy will be identified and measured using cadaver experiments. A mathematical model will be implemented using these error metrics and verified in a simulated environment.

A. CADAVER EXPERIMENTS

Cadaveric experiments were conducted as detailed in Table 1 to measure and record the noise parameters present during an arthroscopy. Cadavers were selected similar in age and knee condition of the typical knee arthroscopy patients surgeons will work on in the theatre. Noise parameters include (1) angular measurement errors calculated by segmenting the instrument gap in the arthroscope images and (2) translation and rotational errors in measuring the arthroscope motion with an OptiTrack system. These errors are analysed to assess the feasibility and robustness of the proposed instrument gap measurement technique for arthroscopy.

TABLE 1. Cadaver experiments to record and calculate image segmentation and translation errors, of a typical knee arthroscopy patient in age and condition.

Experiment	Cadaver	Sex	Age
1	Left and Right Knees	Male	80-90
2	Left and Right Knees	Male	60-70
3	Left and Right Knees	Female	50-60

B. OPTICAL TRACKING

An OptiTrack[1] motion capture system is used during cadaver and laboratory tests to measure the leg movement and arthroscope translation and rotation. Figure 3 shows the setup where ten high-resolution cameras are used to reliably monitor the OptiTrack markers placed in the environment. Our motion capture system runs at up to 120 frames per second (fps), with a resolution of 1280 × 1024 pixels for each of the 1.3 megapixels flex 13 cameras. The system can provide the precision of less than one millimetre when used in a

[1] http://optitrack.com/

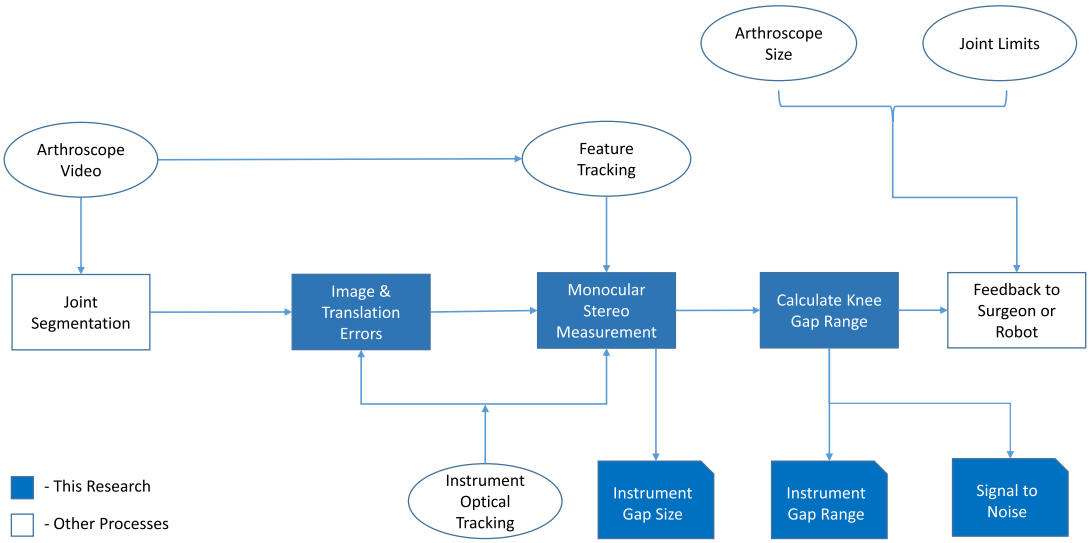

FIGURE 2. Instrument gap Measurement process for this research. From segmented frames the image error is calculated and with the translation errors, the uncertainty in the motion stereo measurement calculated.

FIGURE 3. Optical Tracking volume setup for Cadaver experiments. Ten cameras (the visible cameras is highlighted in yellow) are fitted to a frame that was setup around the cadaver. Cameras were installed at specific points to ensure visibility of the arthroscope from at least three cameras during surgery. Blanking screens are installed to limit reflections.

set environment. Cadaver experiments were performed at the Queensland University of Technology's Medical and Engineering Research Facility (MERF). The system is calibrated with a high precision 250mm wand and a three-marker precision ground plane, to provide an accurate world frame for the experiments.

C. ARTHROSCOPE IMAGES

The Stryker arthroscope used for this research uses the same optical path to provide light into the knee joint to record video of the inner knee [28]. It has a field of view (FOV) of 90° at an angle of 30° at the tip. The video frame rate for the arthroscope camera is 60 frames per second, with a full resolution of 1280 × 720 pixels for each frame.

D. SIMULATION

The Matlab (R2018b) simulation uses two known (or in our case inferred) instrument gap 'features', as well as realistic noise injected into the motion and angular measurements. These noise sources are selected by analysing data from the three Cadaver experiments using the experimental configuration described above. It provides the basis of our validation to measure the instrument gap uncertainty in the presence of sensor errors during surgery. The additional noise-induced due to image irregularities in the form of fat, tissue and water are inherent in the segmentation accuracy analysis that was measured from ten, one hundred images data sets recorded during the cadaver experiments.

E. IMAGE ERRORS

The knee joint has many diagnostic points (typically fifteen) used during arthroscopy, and each of these points has different features, colour and lighting, resulting in a specific image error for that area. From the cadaver data sets, one thousand frames were segmented and manually marked-up by an expert surgeon as a ground truth. Comparing segmentation results utilising the algorithm by Strydom *et al.* with the arthroscope image ground truths, the root mean square (RMS) image errors can be calculated in pixels. Figure 4a details an example of how the errors were measured from the images and the angular image error calculated. With the arthroscope specifications as detailed in section II-C, the degrees per pixel (DPP) in each direction are calculated with:

$$DPP_x = \frac{Max\_Azimuth}{Image\_Width} = 0.075\ [^0/px]$$

$$DPP_y = \frac{Max\_Elevation}{Image\_Height} = 0.125\ [^0/px]$$

With the total image error a combination of these.

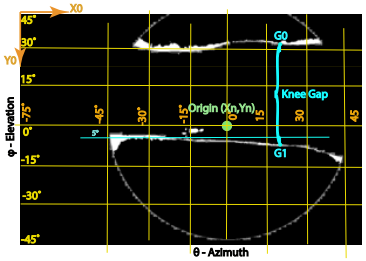

(a) Angular Error within knee gap. For the arthroscope the azimuth and elevation both is 90^o. Due to the 30^o offset angle of the tip, the direction of the movement (where the gap is, is not is the image centre. Image errors from segmentation are the white areas.

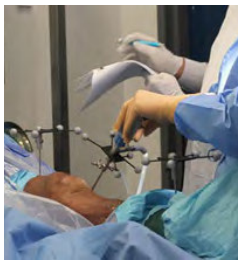

(b) Markers on the Arthroscope and Cadaver leg during Experiment at MERF. The markers on the arthroscope rigid body ensure visibility at all times from the ten tracking cameras.

FIGURE 4. Segmentation errors and Arthroscope tracking.

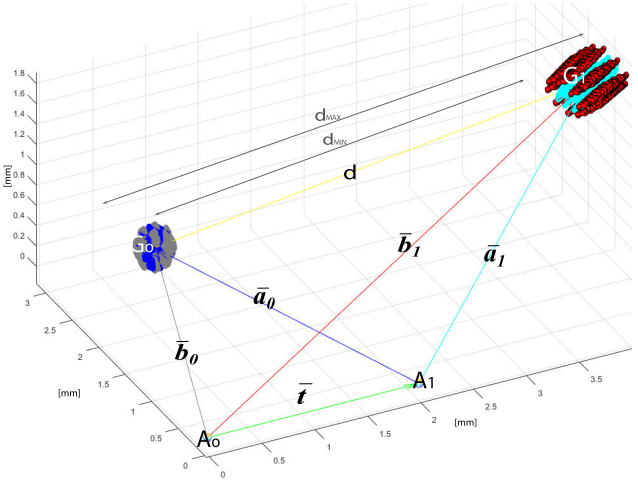

FIGURE 5. Output format for vectors between Instrument gap (G_0 and G_1) and Arthroscope translation points (A_0 and A_1) with Cloud points formed around each gap point from each of the vector pairs.

F. ARTHROSCOPE MOTION ERRORS

Since the arthroscope motion is required to triangulate and calculate the instrument gap size, the measurement accuracy of the motion from one frame to another has a direct impact on computing the instrument gap. For this study, an optical tracking system (section II-B) is used for measuring the translation and rotation of the arthroscope, as shown in Figure 4b. There are many options for measuring the translation, such as using magnetic sensors or high-quality inertial measurement unit systems, all with different error metrics. If improperly set up, the OptiTrack Motive system can significantly skew the subten millimetre range of the instrument gap. For these type of systems, the number of cameras and calibration of the system largely define the accuracy and precision. For the cadaver experiments in this study, ten cameras were used (Figure 3) to ensure robust coverage and precise tracking of the markers between frames during the surgery. To determine the OptiTrack system precision, stationary and moving markers were analysed during cadaver experiments and each of the root mean square (RMS) errors calculated for five sets of over six thousand measurements. The error vector lengths from these measurements provide accurate metrics to establish the error volume due to inherent translation errors during arthroscope movement.

G. ERROR CLOUDS

Error clouds are calculated to measure the instrument gap uncertainty, however the following convention needs to be defined or inferred from Figure 5: a) the instrument gap from G_0 to G_1 b) the 3D translation vector $\vec{\mathbf{t}}$ between points A_0 and A_1 and c) the unit vectors to the edges of the instrument gap $\hat{\mathbf{a}_0}$, $\hat{\mathbf{a}_1}$, $\hat{\mathbf{b}_0}$ and $\hat{\mathbf{b}_1}$, with angles as shown. Each vector configuration has an error volume result – the two error volume pairs are formed from $\vec{\mathbf{a}_0}$, $\vec{\mathbf{a}_1}$ and $\vec{\mathbf{b}_0}$, $\vec{\mathbf{b}_1}$, around each gap point respectively. For the test cases, the vector configuration from the instrument gap (G_0 and G_1) relative to the translation path of the arthroscope (A_0 and A_1) is varied to determine the impact of the translation direction on the error volume.

H. VALIDATION SCENARIOS

To determine the feasibility of our approach to measure the instrument gap, the following scenarios were tested:

1) Translation is perpendicular to the line projected onto the x-y plane joining the two gap locations
2) Translation is 45 degrees to the line projected onto the x-y plane joining the two gap locations
3) Translation is 30 degrees to the line projected onto the x-y plane joining the two gap locations
4) Translation is parallel to the line projected onto the x-y plane joining the two gap locations
5) Parameters the same as in scenario 2; however, in this scenario, both the translation and image errors have been set to the maximum values measured to demonstrate a worst-case scenario.
6) Parameters the same as in scenario 5; however, in this scenario, both the translation distance is increased from 2mm to 8mm to determine the change in uncertainty with an increase in translation distance.
7) Parameters are the same as scenarios 1. However, the translation distance is varied from 0.1mm to 8mm to determine the SNR graph.

Scenarios 1-5 are validated over one thousand runs with randomised translation and angular errors to highlight the overall accuracy of the approach. During these scenarios, the instrument gap and translation distance were held constant. The variation in the angle of incidence is deliberate to determine the effect it has on the measurement accuracy. The instrument gap positions were set at 4mm for G_0 to G_1 to simulate an actual arthroscope size. The arthroscopes translation magnitude was set to 2mm, with the vector starting at (-T sin(ρ)-T cos(ρ)) and ending (0, 0, 0)mm. The final scenario demonstrates the signal to noise ratio (SNR) relationship of the gap size compared to the translation distance when the incidence angle is 45° and 90° degrees. The instrument gap size was held constant during scenario 6. However,

the translation distance was varied. Parameter values used for the simulations were measured during cadaver experiments.

III. THEORY

In this section we derive the equations necessary to measure the distance between two points in the instrument gap. This mathematics will form the basis for the error analysis in the following section.

The errors associated with the arthroscope measurement will be calculated and a mathematical model developed that presents the instrument gap size as a range, where the minimum distance is significant to ensure that the arthroscope can pass through the gap and the maximum distance limits movement of the leg relative to the patients anatomy.

A. MEASURING THE KNEE JOINT

Once the translation vector and instrument gap direction vectors are known, the vectors from the camera position as detailed in Figure 6, to the instrument gap coordinates are calculated from the Sine rule:

$$\vec{a}_n = ||\vec{t}|| \frac{\sin \alpha_n}{\sin \gamma_n} \hat{a}_n \tag{1}$$

$$\vec{b}_n = ||\vec{t}|| \frac{\sin \beta_n}{\sin \gamma_n} \hat{b}_n \tag{2}$$

where n represents either the initial or final coordinate (i.e. $n = 0$ or 1). The vector angles, α_n, β_n and γ_n and the distance d between the two edges of instrument gap are:

$$\alpha_n = \arccos\left(\frac{\vec{t}}{||\vec{t}||} \cdot \hat{b}_n\right) \tag{3}$$

$$\beta_n = \arccos\left(-\frac{\vec{t}}{||\vec{t}||} \cdot \hat{a}_n\right) \tag{4}$$

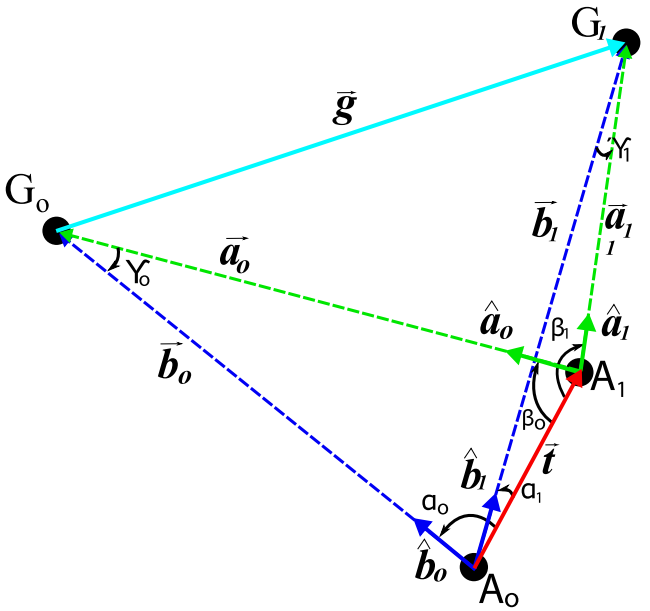

FIGURE 6. Measuring the instrument gap represented by point G_0 and G_1 from camera positions A_0 and A_1, with $\vec{t}$ the translation of the arthroscope.

$$\gamma_n = \pi - (\alpha_n + \beta_n) \tag{5}$$

$$d = ||\vec{g}|| = ||\vec{a}_1 - \vec{a}_0|| = ||\vec{b}_1 - \vec{b}_0|| \tag{6}$$

We have now shown that the distance can be computed using a known translation and the direction vectors to the instrument gap coordinates. The next step is to understand the sensitivity characteristics and derive the errors for imperfect measurements.

B. ERROR ANALYSIS

In this section, we derive the error analysis to form an understanding for how the errors in the measurements of $\vec{t}$, $\hat{a}_0$, $\hat{a}_1$, $\hat{b}_0$ and $\hat{b}_1$ affect the accuracy (or error range) of d. The error analysis will enable us to calculate the gap range, where the arthroscope size (4mm) will relate to the minimum distance, and the maximum is limited by the largest motion of the patient's joint.

Indeed, the two key measurement errors are: (1) the optical tracking rotation and translation errors and (2) the error in the direction vectors to the instrument gap coordinates. These errors induce a variance in the calculated vector lengths and directions (i.e. errors in $\hat{a}_0$, $\hat{a}_1$, $\vec{b}_0$ and $\vec{b}_1$), which ultimately creates an error volume with an offset close to points G_0 and G_1 in Figure 7. Therefore, the error analysis will first derive the variation of the magnitude of $\vec{b}_n$, then the angular error due to segmentation and translation rotational errors. From these, the instrument gap error volume is computed, as well as the signal to noise for the instrument gap measurement.

1) INSTRUMENT GAP VECTORS LENGTH SENSITIVITY

We have shown previously that (in this section we use $\vec{b}_n$ for the derivation):

$$\begin{aligned}\vec{b}_n &= ||\vec{t}|| \frac{\sin \beta_n}{\sin \gamma_n} \hat{b}_n \\ &= ||\vec{t}|| \frac{\sin \beta_n}{\sin (\alpha_n + \beta_n)} \hat{b}_n\end{aligned}$$

If we let the magnitude of $\vec{b}_n$ (or $\vec{a}_n$) be L and the magnitude of the translation ($\vec{t}$) be τ, then:

$$L = \tau \frac{\sin \alpha_n}{\sin (\alpha_n + \beta_n)} \tag{7}$$

The variation in L, ΔL is then:

$$\Delta L = (\tau + \Delta\tau) \frac{\sin (\alpha_n + \Delta\alpha_n)}{\sin (\alpha_n + \Delta\alpha_n + \beta_n + \Delta\beta_n)} - L \tag{8}$$

$$\leq (\tau + \Delta\tau) \frac{\sin \alpha_n + \Delta\alpha_n}{(1 + \frac{\Delta\gamma_n}{\sin \gamma_n}) \sin \gamma_n} - L$$

$$\leq (\tau + \Delta\tau) \left[\left(\frac{\sin \alpha_n}{\sin \gamma_n} + \frac{\Delta\alpha_n}{\sin \gamma_n} \right) \left(1 - \frac{\Delta\gamma_n}{\sin \gamma_n} \right) \right] - L \tag{9}$$

Terms denoted with Δ are small perturbations in the measurements and the worst case is considered from equations (8) to (9) where: $\Delta\alpha_n \cos \alpha_n \leq \Delta\alpha_n$. Equation (9) can

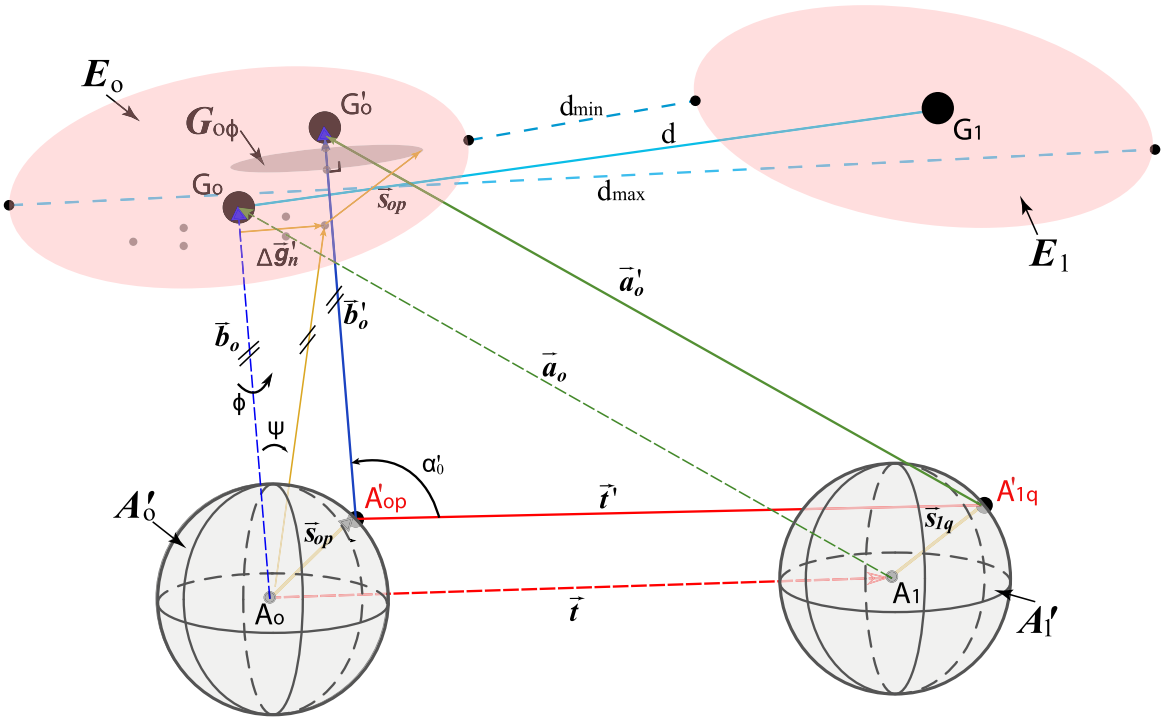

FIGURE 7. Error Volume, where the translation is $\vec{t}$ and the error translation vector array $\vec{t}'$. The resulting translation error volumes A'_0 and A'_1 is surrounding A_0 and A_1. The total angular error (ψ) is the sum of the image (θ) and arthroscope rotational error (ω). E_0 and E_1 are the final error volumes (shown as the red shaded area) around the two instrument gap points G_0 and G_1.

be rewritten as:

$$\Delta L = \tau\frac{\sin\alpha_n}{\sin\gamma_n} - \tau\Delta\gamma\frac{\sin\alpha_n}{\sin^2\gamma_n} + \tau\frac{\Delta\alpha_n}{\sin\gamma_n} + \Delta\tau\frac{\sin\alpha_n}{\sin\gamma_n} - \Delta\tau\Delta\gamma_n\frac{\sin\alpha_n}{\sin^2\gamma_n} + \Delta\tau\frac{\Delta\alpha_n}{\sin\gamma_n} - L \quad (10)$$

Note that in (10) $L = \tau\sin\alpha_n/\sin\gamma_n$ and that second order terms are dropped (i.e. any two small perturbations in measurements multiplied by one another).

$$\Delta L = \tau\left(\frac{\Delta\alpha_n}{\sin\gamma_n} - \frac{\Delta\gamma_n\sin\alpha_n}{\sin^2\gamma_n}\right) + \Delta\tau\frac{\sin\alpha_n}{\sin\gamma_n} \quad (11)$$

It is apparent from (11), that as γ_n (or $\alpha_n + \beta_n$) approaches 90°, ΔL reduces to a minimum. For a very short translation distance, that is where γ_n approaches zero, ΔL become large and the error overshadows the measurement. The translation error changes $\vec{t}$ have an effect on the angles α_n and β_n, which then change L by ΔL (11), with the Δ values of these angles. However as we have selected the gap for the simulation and translation points, we can calculate the error in L using these points as ground truth. During an arthroscopy this will not be possible as the actual measurement is unknown.

$$L_{error} = L_{GT} - (L + \Delta L) \quad (12)$$

2) ERROR VOLUMES

The purpose of this section is to identify the potential errors induced through measurement and use that to calculate the error volumes. Specifically, three sets of errors are introduced through measurement conditions: (1) the error in α_n and β_n due to the arthroscope translation measurement, (2) the arthroscope rotational error (ω) around $\vec{a}_n$ and $\vec{b}_n$ and (3) the angular image error (θ) around the computed direction vectors, $\hat{a}_n$ and $\hat{b}_n$.

First the errors due to the translation are derived. For simplicity, we define the translation measurement error as a spherical volume surrounding A_0 and A_1, with radius ΔT. Therefore, the start and end points of the translation vector can lie anywhere within these two volumes, respectively, as shown in Figure 7. To determine the effects of the translational error on the final gap error volumes, we need to determine the effect of 'all' translation vector start and end points.

A'_0 is an array that donates all the possible starting points for $\vec{t}'$ and $\boldsymbol{A'}_1$ an array that donates all the possible end points for $\vec{t}'$, where:

$$\boldsymbol{A'}_0 = \hat{\boldsymbol{r}}_{(az,el)}\Delta T \quad (13)$$

$$\boldsymbol{A'}_1 = \vec{\boldsymbol{t}} + \hat{\boldsymbol{r}}_{(az,el)}\Delta T \quad (14)$$

ΔT, the translational measurement error, is the measurement precision of the arthroscope translation tracking and randomly varies from zero to a maximum translation error. It is used to scale the unit vector $\hat{\boldsymbol{r}}$, where:

$$\hat{\boldsymbol{r}}_{(az,el)} = \begin{pmatrix} \sin(az)\cos(el) \\ \cos(az)\cos(el) \\ \sin(el) \end{pmatrix} \quad (15)$$

The azimuth (az) has a range of $(-\pi, \pi)$ and elevation (el) has a range of $[-\pi/2, \pi/2]$. Both A'_0 and A'_1 is a spherical surface for a constant ΔT, however as ΔT varies within the measurement system's precision range, an error volume is created around A_0 and A_1 as seen in Figure 7 as the grey shaded area.

The numerous potential translation vectors $\vec{t}'$, are calculated through iterating through each set of two points p and q in the two translation error volumes A'_0 and A'_1 respectively. The arrays A'_0 and A'_1 defines an combination of translation vectors so that:

$$\vec{t}'_{p,q} = A'_{1q} - A'_{0p} \text{ where } \begin{cases} p = 1, 2, \ldots P \\ q = 1, 2, \ldots Q \end{cases} \tag{16}$$

where P and Q is the number of points in A'_0 and A'_1 respectively. With the angular error (ψ), the new translation vector array creates a new set of α_n and β_n angles such that:

$$\alpha'_n = \arccos(\hat{t}'_{p,q} \cdot \hat{b}_n) \pm \psi \tag{17}$$

$$\beta'_n = \arccos(-\hat{t}'_{p,q} \cdot \hat{a}_n) \pm \psi \tag{18}$$

These α'_n and β'_n angles can be used to calculate the $\Delta\alpha_n$ and $\Delta\beta_n$ errors, which are required for (11) to determine ΔL for calculation of the final error volumes (E_0 and E_1) around G_0 and G_1.

$$\Delta\alpha_n = \alpha_n - \alpha'_n \tag{19}$$

$$\Delta\beta_n = \beta_n - \beta'_n \tag{20}$$

3) ERROR VOLUMES FOR KNEE ARTHROSCOPY

Image gap measurement errors (θ) and arthroscope rotational errors (ω) both present as angular errors around $\hat{a}_n$ or $\hat{b}_n$ and with the total error range, $\psi = \pm(\theta + \omega)$. Through using the derived errors in the previous sections, the final error volumes around the two instrument gap points E_0 and E_1, can be calculated with:

$$E_0 = A'_0 + G_{0\phi} \tag{21}$$

$$E_1 = A'_1 + G_{1\phi} \tag{22}$$

$G_{n\phi}$ is the array of point we obtain when rotating $\Delta\vec{g}_n$ around $\vec{a}_n$ or $\vec{b}_n$ and then translating with $\vec{s}_n$, the vectors from A_o to A'_{op} and A_1 to A'_{1q}

With a magnitude for $\Delta\vec{g}_n$ of:

$$||\Delta\vec{g}_n|| = (L + \Delta L)\sin\psi \tag{23}$$

where $L = ||\vec{b}_n||$, and the direction of $\Delta\vec{g}_n$ is:

$$\Delta\hat{g}_n = \frac{\left[\hat{b}_n \times (\hat{t}'_{pq} \times \hat{b}_n)\right]}{\left|\left|\left[\hat{b}_n \times (\hat{t}'_{pq} \times \hat{b}_n)\right]\right|\right|} \tag{24}$$

so that:

$$\Delta\vec{g}_n = \frac{\left[\hat{b}_n \times (\hat{t}'_{pq} \times \hat{b}_n)\right]}{\left|\left|\left[\hat{b}_n \times (\hat{t}'_{pq} \times \hat{b}_n)\right]\right|\right|}(L + \Delta L)\sin\psi \tag{25}$$

We find the instrument gap; which takes into account the measurement errors; between two set of error cloud points:

$$d_e = E_{1i} - E_{0j} \quad \text{and} \quad \begin{cases} i = 1, 2, \ldots I \\ j = 1, 2, \ldots J \end{cases}$$

With the signal to noise ratio of the instrument gap:

$$SNR_d = \frac{d}{d_{e(max)} - d_{e(min)}} \tag{26}$$

For simulation the variables are selected in the following ranges and with step sizes as specified:

el	$[-\frac{\pi}{2}, \frac{\pi}{2}]$	el steps:	[4]
az	$[-\pi, \pi]$	az steps:	[6]
$\boldsymbol{t}$	[Constant]	ΔT steps:	[0.01 : 0.3]
ϕ	$[-\pi, \pi]$	ϕ steps:	$[0, \frac{\pi}{6}, \frac{\pi}{4}, \frac{\pi}{2}]$
$\pm\omega$	[Constant]		
$\pm\theta$	[Constant]		

C. IMPLEMENTATION FOR RELIABLE MEASUREMENTS

The SNR_d ratio can be used to decide if more translation is required or if the gap is defined to an adequate degree to decide on a specific action for the operator. The level for SNR_d will need to be set for a specific procedure and conditions to ensure successful transition to a specific part of the knee.

The analysis can be viewed from both the $\vec{a}_n$ or $\vec{b}_n$ or a combination can be used to determine the best SNR_d value.

IV. RESULTS

In this section the results are provided for the six test cases in a format as detailed in Figure 5 and 7.

A. IMAGE ERRORS

The instrument gap was segmented for a thousand images selected from different regions of the knee and compared against images marked-up by an expert surgeon as seen in Figure 8 [4].

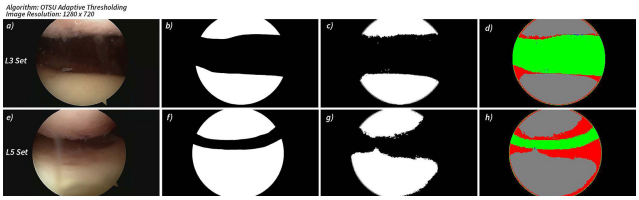

FIGURE 8. Segmentation and image Errors of the instrument gap for two areas inside the knee joint using the OTSU algorithm: (a,e) Arthroscope Video frame, (b,f) Marked-up Image, (c,g) OTSU Mask, (d,h) SAD output with image errors FP (red) and FN (blue).

The difference image (Figure 8(d)) is colour coded to highlight the True Positives (TP-Green), True Negatives (TN-Grey), false Positives (FP-Red) and False Negatives (FN-Blue) from the segmentation results. The calculation of the image angular error (ψ) is then computed, as the angular resolution of each pixel is known.

The average image errors (θ) was calculated as detailed in Table 2 for selected diagnostic points inside the knee. The medial compartment is one of the first spaces seen during an arthroscopy and its image error (item 2) of 2.36° will be used for detailed analysis in this study.

TABLE 2. Image errors at specific diagnostic points inside the knee joint. Errors around the two gap points are calculated, with the average between these points provided.

No	Image Set	Location Inside the Knee Joint	G_0 Gap Error	G_1 Gap Error	Ave Image Error
1	2	Medial Compartment	5.215	3.388	4.302
2	3	Patellar Femoral Joint	1.961	2.774	2.367
3	6	Lateral Compartment	4.048	7.125	5.586

B. TRANSLATION ERRORS

The RMS error for the Optitrack translation (ΔT) is 0.0367mm recorded over all the ten data sets. The average arthroscope rotational error (ω) is 0.03° over the data sets. The translation measured during the cadaver experiments are detailed in Table 3.

TABLE 3. Simulation Parameters. Set 1 is the average errors, set 2 the maximum measured translation and image errors, set 3 with a fixed 8mm translation and with set 4 the translation distance is varied.

Set	Translation Angles	ΔT [mm]	Gap [mm]	t [mm]	θ	ω
1	0^o,30^o, 45^o,90^o	0.0367	4	2	2.36^o	0.004^o
2	45^o,	0.0698	4	2	5.586^o	0.177^o
3	45^o,	0.0698	4	8	5.586^o	0.177^o
4	90^o,	0.0367	4	0.1:0.1:8	2.36^o	0.004^o

C. ERROR CLOUDS

Figures 9a and 10 are the results for scenarios one to five (from 0° to 90°) for the cloud points with vectors, and Figure 9b the delta L error for zero degrees translation (12). The results from these figures are shown in Table 4, using parameters as detailed in Table 3 (Set 1).

Scenarios 5 and 6 in Table 4 are presented in Figure 11 and are the results for the maximum measured error ranges (Table 3 – Set 2 and 3) and emphasise translation distance influence on the error point cloud. Table 4 includes the gap for various angles, and the mean and standard deviation error of the motion stereo over one thousand test runs. The uncertainty was calculated from the point cloud extremes and the average gap over the thousand runs provided for each translation angle (each with a random translation and angular error bounded by the parameters outlined in Section II-B).

Figure 12 presents scenario six and is the instrument gap size signal to noise (SNR_d) ratio as frames are translated during the procedure.

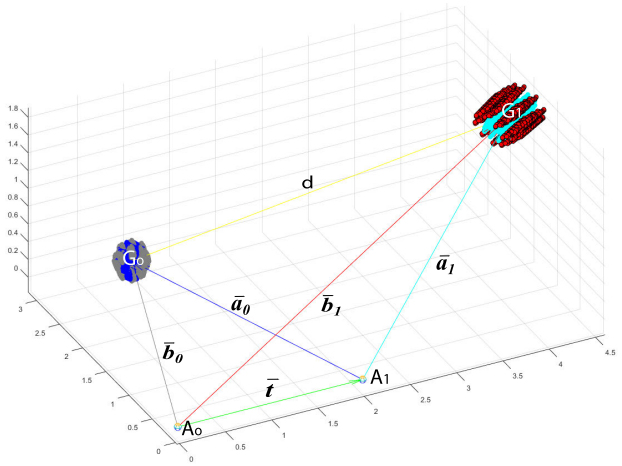

(a) Point Cloud around each Gap point, with a fixed translation distance of 2mm and gap of 4mm.

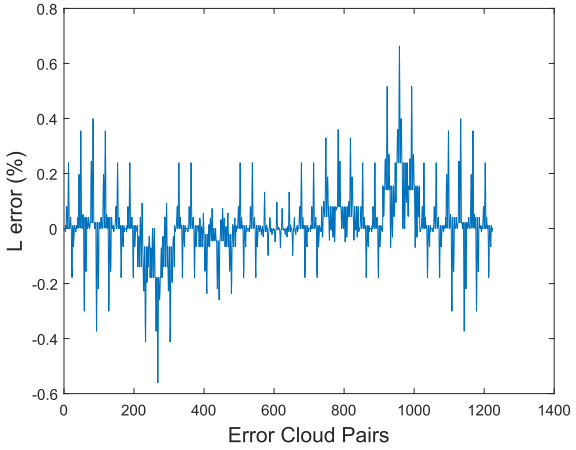

(b) The L Error showing the variation of $\Delta L + L$ from the ground truth Length for L.

FIGURE 9. Cloud points at 0° Translation.

V. DISCUSSION

As the arthroscope moves through the knee during surgery, it is necessary to constantly adjust the patient's leg position to create the appropriate space for the surgical equipment. The anatomical joint safe range (or upper limits) of the patient is known to control the maximum force that can be applied to a joint at each leg position. Surgeons currently "feel" the limb resistance. In conjunction with 'feeling' the force they apply to the leg, surgeons further estimate the joint space from a 2D video steam in front of them. In many cases, they over or underestimate the instrument gap, resulting in damaging to the knee joint by applying excessive force to it or pushing the instrument through a gap that is too small. Computer vision is ideally placed to reduce trauma to patients, by measuring this "instrument gap" and provide feedback to the operator, whether it is a robot or surgeon. This research presents an algorithm to determine the uncertainty or range of measuring the instrument gap inside the

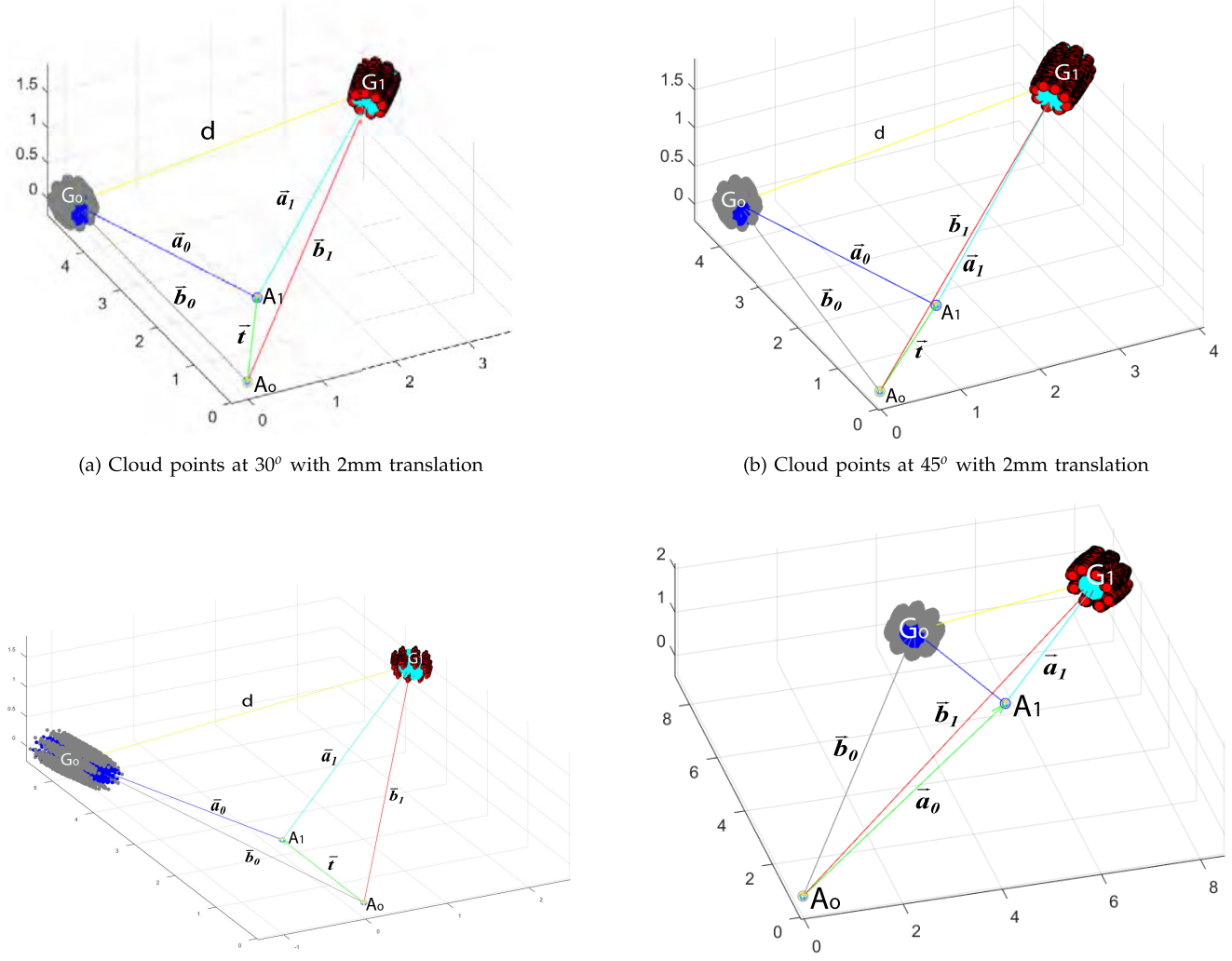

(a) Cloud points at 30^o with 2mm translation

(b) Cloud points at 45^o with 2mm translation

(c) Cloud points at 90^o with 2mm translation

(d) Cloud points at 45^o with 8mm translation

FIGURE 10. Translation Point Clouds around the gap of 4mm.

TABLE 4. Instrument gap Error Analysis Results with scenario one to four (set 1) the measurements from changing the translation angle (using image set 2). Scenario five (set 2) use 2mm translation with the maximum measure errors at 45° for both translation and image. Scenario six (set 3) used the same parameters as scenario 5, but with a 8mm translation and in scenario 7 the translation is varied from 0.1mm to 8mm to plot the SNR graph.

Parameter Set	Translation Angle	Uncertainty (Range) Min	Max	Gap Measurement Error Mean	Std Dev	Scenario #
1	0^o	3.351	4.724	-0.0052	0.0147	1
	30^o	3.492	4.525	-0.0032	0.0086	2
	45^0	3.346	4.562	-0.0067	0.0052	3
	90^0	3.515	4.497	0.0221	0.0054	4
Average Set 1		3.426	4.577	0.0018	0.0085	
2	45^0	2.875	5.256	-0.019	0.0016	5
3	45^0	3.525	4.495	0.0063	0.0013	6
4	90^0	SNR Graph				7

knee joint. It is a minimum where surgical tools need to pass through and a maximum at the joint motion limits.

Optical sensor and image processing noise were measured during cadaveric experiments and used to verify the approach through simulation. The results show that under perfect conditions and using motion stereo, we can accurately measure the instrument gap. However, a high level of uncertainty is introduced with the image processing and arthroscope motion

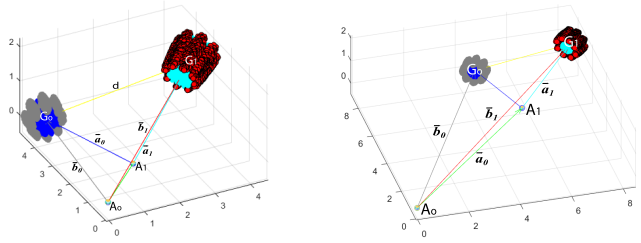

(a) 2mm Translation. (b) 8mm Translation.

FIGURE 11. The impact of an increase translation from 2mm to 8mm, with parameters as detailed in Image sets 2 and 3 in Table 3). The translations are at 45°, with a instrument gap of 4mm and a ΔT of 0.0698mm.

measurements, impacting the actual instrument gap measurement by ±14%.

The results in Table 4 demonstrates that motion stereo accurately measures the instrument gap. The average of the measurements has a mean of -0,0028mm and standard deviation of 0.0096mm. These results are well within the accuracy range that can be achieved by surgeons or robots. However, from cadaver measurements, significant noise is present in the form of image segmentation and translation measurements errors that influences the motion measurements. These errors were analysed, and algorithms developed to measure the uncertainty range of the instrument gap.

The range measurement is defined by the errors inherent to an arthroscopy setup and conveniently reflects the two extremes for any surgery: (1) the minimum size required for the arthroscope to pass through the space safely and (2) the maximum gap size due to the human's anatomical limit. A practical outcome of this research is that the uncertainty range has can effectively be used as a guide during the surgery. Cadaver experiments, as detailed in Table 1 were used to analyse the relevant image and translation errors.

Images errors from segmentation were converted to spherical coordinates, and from Table 2 these errors are significant and have an impact on the uncertainty range. The OTSU segmentation method used is fast and with an adequate level of accuracy [4], providing a good indication of how the identification of the instrument gap influences the gap measurement accuracy. However, in developing techniques such as using deep learning algorithms [29], these errors will reduce over time, improving the overall uncertainty range of the instrument gap measurement.

Tracking the arthroscope introduced translation and rotation errors as presented in Table 3 that form point clouds around the translation points and vectors to the instrument gap. Optical tracking precision is high, with the translation error 0.0367mm. However, it has an amplification impact on the rotational error volumes, translating them in all directions around the gap points. The optical tracking rotational error is insignificant (0.004°) and negligible in comparison to the image error.

Error volume results in Figure 9a to 10c show that images with a combination of rotation and translation errors and different translation directions have different error point clouds surrounding the two gap points. Each volume is relative to a set of vectors ($\vec{a}_0$ and $\vec{b}_0$ or $\vec{a}_1$ and $\vec{b}_1$) and is independent in shape and size due to the unique noise and error characteristics of each triangulation vector. Indeed, the best combination of the four error volumes can be used for feedback and control purposes. The minimum and maximum instrument gap range values calculated from these point clouds are presented in Table 4, for the four translation angles (using $\vec{b}_n$). The larger the image and translation errors, the larger the volumes as shown for 45° between figures 10b and 10d.

The results in Table 4 shows the best angle to be 45° and that in general, the higher angles are slightly worst than the lower angles. The change is marginal, and the translation angle doesn't have a significant impact (maximum 0.169mm) on the uncertainty range. The actual gap size was set at 4mm during the simulation and indicated that by taking into account the uncertainty, the gap size is underestimated by 13.91% and overestimated it by 14.03% as shown in Table 4. The total uncertainty range is on average 1.1172mm or 27% of the actual gap size. At the minimum side, we thus need to increase the gap until it is more than 4mm to ensure the arthroscope can safely pass through, however, the anatomical limits of the patient's joint needs to be considered.

Using a signal to noise approach it is possible to change the measurement accuracy through controlling the arthroscope translation distance as shown by the signal to noise graphs in Figure 12 and the resulting cloud volumes in figure 11. The potential benefit of the SNR_d value is that it provides a single metric to determine the accuracy of the gap measurement. The length of the $\vec{a}_n$ or $\vec{b}_n$ vectors depends on the gap position and the initial and final translation points. These vector lengths change the size of the error clouds, and different vector combinations will result in a higher or lower SNR_d. Using this SNR_d graph, a threshold can be set at the desired noise level for a specific surgical procedure. Once the desired noise to signal is reached, the measurement values are within the predefined tolerances for the surgery. Larger error volumes for the same translation lower the SNR_d, reducing the accuracy and control range as shown between Figures 12a and 12b.

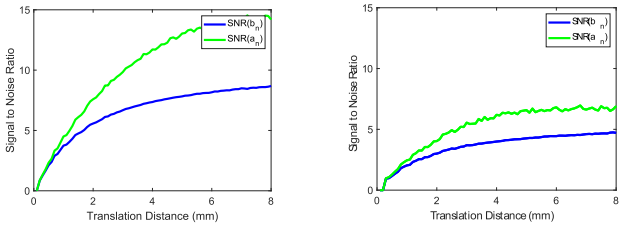

(a) Signal to Noise Ratio with the errors as per set 2 in Table III, with 2mm translation.

(b) Signal to Noise Ratio with errors as per set 3 in Table III, where we translated 8mm.

FIGURE 12. Signal to Noise Ratios of the measured gap distance (ground truth distance) compared to gap range, using the calculated error cloud uncertainty.

A. LIMITATIONS

Limitations of this study include tracking of the anatomical points of interest inside the knee joint that forms the instrument gap over multiple frames. It is also necessary to investigate the full effects of changes in translation and image errors during an arthroscopy (such as when the arthroscope bends).

B. APPLICATIONS

The primary focus of this research is to calculate the noise parameters during motion stereo measurement of the instrument gap to determine the uncertainty in the gap size. Using imperfect state information in real environments (from low cost or existing sensors), can be used to provide sufficient information for a range of applications, including:

- Measuring system inside the knee joint using a standard arthroscope for surgeon feedback, or robotic applications during automated knee arthroscopy
- Minimal invasive surgery of other joints in the body
- Land and under any water robotic applications to accurately measure range with motion cameras, while characterising the uncertainty

VI. CONCLUSION

Measuring the surgical space inside the knee joint for minimally invasive surgery has significant benefits for both the patient and surgeon. This study contributes to the mathematical development of the uncertainty in image and arthroscope motion errors during motion measurement of the joint. Our results show that using computer vision, images from a standard arthroscope can be used to measure the instrument gap and calculate the uncertainty range of the measurement. The gap size and uncertainty range can be used to provide feedback to a surgeon while moving surgical instruments through the knee joint or enable control of a robotic leg manipulator.

This is the first study to identify internal knee joint parameters and to model the instrument gap range for knee arthroscopy. It forms the bases for future work to:

- Track the instrument gap points in a human joint from one frame to another during an arthroscopy
- Use the algorithms and parameters developed in this study to measure the joint during arthroscopy in real-time

ACKNOWLEDGMENT

The authors would like to acknowledge the Advanced Queensland Scheme and the Queensland University of Technology Research Training Program funding support, thank Andres Marmol-Velez for his assistance during cadaver tests, Reuben Strydom for technology discussions reviewing this study and Thomas Coppin for reviewing the mathematics.

Cadaveric experiments were approved by the Australian National Health and Medical Research Council (NHMRC) - Committee no. EC00171, Approval no. 1400000856.

REFERENCES

[1] B. P. McKeon, J. V. Bono, and J. C. Richmond, *Knee Arthroscopy*. New York, NY, USA: Springer, 2009.

[2] S. Rasool and A. Sourin, "Image-driven virtual simulation of arthroscopy," *Vis. Comput.*, vol. 29, no. 5, pp. 333–344, May 2013.

[3] B. D. Ward and J. H. Lubowitz, "Basic knee arthroscopy part 3: Diagnostic arthroscopy," *Arthroscopy Techn.*, vol. 2, no. 4, pp. e503–e505, Nov. 2013.

[4] M. Strydom, A. Jaiprakash, R. Crawford, T. Peynot, and J. M. Roberts, "Towards robotic arthroscopy: 'Instrument gap' segmentation," in *Proc. Australas. Conf. Robot. Autom.*, Dec. 2016.

[5] L. Blankevoort, R. Huiskes, and A. de Lange, "The envelope of passive knee joint motion," *J. Biomech.*, vol. 21, no. 9, pp. 705–720, 1988.

[6] A. Jaiprakash, J. M. Roberts, and R. Crawford, "Perceptions of Orthopaedic Surgeons on knee arthroscopic surgery," *J. Orthopaedic Surgery*, to be published.

[7] L. Wu, J. Jaiprakash, A. K. Pandey, D. Fontanarosa, Y. Jonmohamadi, M. Antico, M. L. Strydom, A. Razjigaev, F. Sasazawa, J. Roberts, and R. Crawford, *Robotic Image-Guided Knee Arthroscopy*. Amsterdam, The Netherlands: Elsevier, 2018.

[8] A. Marmol, T. Peynot, A. Eriksson, A. Jaiprakash, J. Roberts, and R. Crawford, "Evaluation of keypoint detectors and descriptors in arthroscopic images for feature-based matching applications," *IEEE Robot. Autom. Lett.*, vol. 2, no. 4, pp. 2135–2142, Oct. 2017.

[9] J. R. Doyle, "The arthroscope, then and now," *Techn. Hand Upper Extremity Surgery*, vol. 12, no. 4, p. 201, Dec. 2008.

[10] K. W. Nam, J. Park, I. Y. Kim, and K. G. Kim, "Application of stereo-imaging technology to medical field," *Healthcare Informat. Res.*, vol. 18, no. 3, pp. 158–163, Sep. 2012.

[11] Stryker. *Mako*. Accessed: Apr. 4, 2019. [Online]. Available: https://www.stryker.com/us/en/portfolios/orthopaedics/joint-replacement/mako-robotic-arm-assisted-surgery.html

[12] D. Stoyanov, M. V. Scarzanella, P. Pratt, and G. Z. Yang, "Real-time stereo reconstruction in robotically assisted minimally invasive surgery," in *Proc. Int. Conf. Med. Image Comput. Comput.-Assist. Intervent.* Berlin, Germany: Springer, Sep. 2010, pp. 275–282.

[13] S. Röhl, S. Bodenstedt, S. Suwelack, H. Kenngott, B. P. Mueller-Stich, R. Dillmann, and S. Speidel, "Real-time surface reconstruction from stereo endoscopic images for intraoperative registration," *Proc. SPIE*, vol. 7964, Mar. 2011, Art. no. 796414.

[14] M. Field, D. Clarke, S. Strup, and W. B. Seales, "Stereo endoscopy as a 3-D measurement tool," in *Proc. Annu. Int. Conf. IEEE Eng. Med. Biol. Soc.*, Sep. 2009, pp. 5748–5751.

[15] R. Nevatia, "Depth measurement by motion stereo," *Comput. Graph. Image Process.*, vol. 5, no. 2, pp. 203–214, Jun. 1976.

[16] M. Ye, E. Johns, A. Handa, L. Zhang, P. Pratt, and G.-Z. Yang, "Self-supervised siamese learning on stereo image pairs for depth estimation in robotic surgery," May 2017, *arXiv:1705.08260*. [Online]. Available: https://arxiv.org/abs/1705.08260

[17] M. Visentini-Scarzanella, T. Sugiura, T. Kaneko, and S. Koto, "Deep monocular 3D reconstruction for assisted navigation in bronchoscopy," *Int. J. Comput. Assist. Radiol. Surg.*, vol. 12, no. 7, pp. 1089–1099, 2017.

[18] D. Chwa, A. P. Dani, and W. E. Dixon, "Range and motion estimation of a monocular camera using static and moving objects," *IEEE Trans. Control Syst. Technol.*, vol. 24, no. 4, pp. 1174–1183, Jul. 2016.

[19] D. Scaramuzza, F. Fraundorfer, M. Pollefeys, and R. Siegwart, "Absolute scale in structure from motion from a single vehicle mounted camera by exploiting nonholonomic constraints," in *Proc. IEEE 12th Int. Conf. Comput. Vis.*, Sep./Oct. 2009, pp. 1413–1419.

[20] R. Mazzon, "Real-time structure from motion for monocular and stereo cameras," in *Proc. 15th IEEE Medit. Electrotech. Conf.*, Apr. 2010, pp. 498–503.

[21] D. Yang, F. Sun, S. Wang, and J. Zhang, "Simultaneous estimation of ego-motion and vehicle distance by using a monocular camera," *Sci. China Inf. Sci.*, vol. 57, no. 5, pp. 1–10, May 2014.

[22] Z. Xu, C. Li, X. Zhao, and J. Chen, "Depth measurement using monocular stereo vision system: Aspect of spatial discretization," *Proc. SPIE*, vol. 7850, Nov. 2010, Art. no. 785020.

[23] L. P. Maletsky, J. Sun, and N. A. Morton, "Accuracy of an optical active-marker system to track the relative motion of rigid bodies," *J. Biomech.*, vol. 40, no. 3, pp. 682–685, 2007.

[24] A. Saxena, J. Schulte, and A. Y. Ng, "Depth estimation using monocular and stereo cues," in *Proc. IJCAI*, vol. 7, Jan. 2007, pp. 2197–2203.

[25] R. Hartley, R. Gupta, and T. Chang, "Stereo from uncalibrated cameras," in *Proc. IEEE Comput. Soc. Conf. Comput. Vis. Pattern Recognit.*, Jun. 1992, pp. 761–764.
[26] R. I. Hartley and P. Sturm, "Triangulation," *Comput. Vis. Image Understand*, vol. 68, no. 2, pp. 146–157, 1997.
[27] P. A. Beardsley, A. Zisserman, and D. W. Murray, "Navigation using affine structure from motion," in *Proc. Eur. Conf. Comput. Vis.* Berlin, Germany: Springer, May 1994, pp. 85–96.
[28] Dahiteb. (2015). *Arthroscopes*. [Online]. Available: http://www.dahiteb.com/products/endoscopy/arthroscopy/arthroscopes.html
[29] G. Litjens, T. Kooi, B. Ehteshami, B. A. A. A. Setio, F. Ciompi, M. Ghafoorian, J. A. W. M. van der Laak, B. Ginneken, and C. I. Sánchez, "A survey on deep learning in medical image analysis," *Med. Image Anal.*, vol. 42, pp. 60–88, Dec. 2017.

MARIO STRYDOM received the bachelor's degree in electronics and a business master. He is currently pursuing the higher degree research with the Australian Centre for Robotic Vision and the Queensland University of Technology. He has published in the research area of image segmentation and has a PCT approved patent for a robotic leg manipulator from the Australian patent office. He has 25 years of industry experience in the field of automation, electronics engineering and information technology. His researches focus on the field of computer vision and robot kinematics applied for medical robotics.

ROSS CRAWFORD received the Ph.D. degree. He is currently a Professor of orthopaedic research with QUT and undertake private clinical practise at the Prince Charles and Holy Spirit Hospitals. He has mentored over 30 Ph.D. and M.Phil. students to the completion of their degrees and has a wealth of experience in teaching and leading researchers at all levels. He is currently a member of numerous medical committees. He has published more than 200 articles. As an expert surgeon, he assists with cadaver surgery experiments at the QUT Medical and Engineering Research Facility at the Prince Charles campus and brings significant knowledge of knee arthroscopy and the use of medical robotics to this research.

JONATHAN ROBERTS received the Ph.D. degree. He is currently a Professor of robotics with the Queensland University of Technology (QUT) and the Principal Supervisor for this research. After many years of industry experience in robotics, he is leading Medical Robotics at QUT. He has held senior positions at the CSIRO. He was the President of Australian Robotics and Automation Association, from 2007 to 2008. He was a member of IEEE Robotics and Automation Society.

ANJALI JAIPRAKASH received the Med.Sc. degree. She is currently a Life Sciences Scientist and an Advance QLD Research Fellow of medical robotics with the Australian Centre for Robotic Vision and the Queensland University of Technology. She works at the intersection of medicine, engineering and design developing medical devices for diagnosis and surgery, including the patented light field retinal diagnostic systems and vision-based robotic leg manipulation system. She has experience in the field of orthopaedic research, optics and design. She has extensive research experience in the hospital and clinical setting and the ethical conduct of research in compliance with the Australian Code for the Responsible Conduct of Research.